

**Amino Acids Critical for Substrate Affinity of Rat Organic Cation
Transporter 1 Line the Substrate Binding Region in a Model Derived
from the Tertiary Structure of Lactose Permease.**

**Christian Popp¹, Valentin Gorboulev¹, Thomas D. Müller, Dmitry Gorbunov, Natalia
Shatskaya, and Hermann Koepsell**

*Institute of Anatomy and Cell Biology (C.P., V.G., D.G., N.S., H.K.) and Institute of
Physiological Chemistry (T.D.M.), Universität Würzburg, Germany*

Running title:

Amino acids in the substrate binding region of rOCT1

Corresponding author:

Hermann Koepsell, Institute of Anatomy and Cell Biology, Koellikerstr. 6, 97070

Würzburg, Germany

Phone: +49 931 312700

Fax: +49 931 312087

E. mail: Hermann@Koepsell.de

Number of text pages (without title pages, abstract, references and legends): 21

Number of tables: 2

Number of figures: 7

Number of references: 26

Number of words in the abstract: 249

Number of words in the discussion: 1439

ABBREVIATIONS: MFS, major facilitator superfamily; TMH, transmembrane α -helix; OCT, organic cation transporter; LacY, lactose permease Y; TEA, tetraethylammonium; MPP, 1-methyl-4-phenylpyridinium; PBS, phosphate buffered saline; TP₄A, tetrapentylammonium.

To identify functionally relevant amino acids in the rat organic cation transporter rOCT1 eighteen consecutive amino acids in the presumed 4th transmembrane α -helix (TMH) were mutated and functionally characterized after expression in oocytes of *Xenopus laevis*. After mutation of three amino acids on successive turns of the α -helix K_M values for tetraethylammonium (TEA) and/or 1-methyl-4-phenylpyridinium (MPP) were decreased. After replacement of W218 by tyrosine (W218Y) and Y222 by leucine (Y222L) the K_M values for both TEA and MPP were decreased. In mutant Y222F only the K_M for TEA, and in mutant T226A only the K_M for MPP was decreased. The data suggest that amino acids W218 and Y222 participate in binding of both, TEA and MPP, whereas T226 is only involved in binding of MPP. Using the crystal structure of the lactose permease LacY from *Escherichia coli* that belongs to the same major facilitator superfamily as rOCT1, we modelled the tertiary structure of the presumed 12 transmembrane α -helices. The validity of the model was suggested since seven amino acids that have been shown to participate in binding of cations by mutagenesis experiments (4th TMH W218, Y222, T226 (this paper); 10th TMH A443, L447, Q448 (accompanying paper); 11th TMH D475 (previous report)) are located in one region surrounding a large cleft that opens to the intracellular side. The dimensions of TEA in comparison to the interacting amino acids in the modelled cleft suggest that more than one TEA molecule can bind in parallel to the modelled conformation of the transporter.

The *SLC22* transporter family, a member of the major facilitator superfamily MFS, comprises polyspecific transporters with twelve presumed transmembrane α -helices (TMH) for organic cations, organic anions and zwitterions (Koepsell et al., 2003; Koepsell, 2004). Three subtypes of polyspecific organic cation transporters have been identified (*SLC22A1-3* or OCT1-3). These transporters are critically involved in the elimination of cationic drugs and metabolic waste products in liver and kidney. OCT1 is mainly expressed in liver where it is localized at the sinusoidal membrane of the hepatocytes (Gründemann et al., 1994; Gorboulev et al., 1997; Meyer-Wentrup et al., 1998). It mediates the first step in biliary secretion of organic cations, i.e. their uptake into hepatocytes. Because the transporters OCT1-3 can transport cations in both directions (Busch et al., 1996; Budiman et al., 2000; Koepsell et al., 2003) OCT1 is supposed to be also responsible for the release of organic cations across the sinusoidal membrane into the blood. Employing nontransported inhibitors in combination with giant patch method we determined ligand affinities of the outwardly and inwardly oriented conformations of the substrate binding region of rat OCT2 (Volk et al., 2003). These data suggest that the binding region of rOCT2 comprises overlapping binding sites for different substrates which differentially alter their affinity during reorientation. This interpretation was supported by the observation that the mutation of aspartate 475 to glutamate in the binding region of rOCT1 led to a drastic increase in affinity for some substrates and competitive inhibitors, but did not influence the affinity of another substrate (Gorboulev et al., 1999).

For the understanding of drug transport and for the design of drugs with optimized biodistribution and excretion, it is important to elucidate the structure of the substrate binding regions of polyspecific transporters of the *SLC22* family, how various substrates bind to these regions, whether more than one substrate can bind simultaneously, and how substrate binding initiates the translocation process. Ultimately, these questions can only

be solved by crystallization of ligand-transporter complexes in combination with functional characterization of point mutations of critical residues.

In recent years, functional effects of many individual point mutations on transport activity and/or substrate affinity of transporters of the *SLC22* family have been described (Koepsell and Endou 2004; Koepsell et al., 2003). It turned out that mutations in several of the presumed twelve membrane-spanning α -helices (TMHs 1,2,4,7,8,11), in the large extracellular loop, and in the large intracellular loop lead to functional changes such as differential affinity changes for various substrates. Considering the possibility that part of these changes may be due to long-range effects on the conformation of the substrate binding region, we reasoned that indirect effects were much less probable if amino acids with specific effects on substrate affinity could be identified in neighbouring positions within the secondary structure, e.g. on one side of an α -helix. For this reason, we carried out a systematic mutational screening of the presumed 4th TMH of rOCT1. We measured transport activity for two different substrates in mutants of 18 consecutive amino acids and investigated 9 of these amino acids in more detail. The 4th TMH was selected because this TMH contains several amino acids on one side of the presumed α -helix that are conserved within the three OCT-subtypes but not in the closely related organic anion transporters. We obtained data indicating that 3 amino acids in neighbouring positions on one side of the presumed 4th TMH participate in substrate binding.

Recently, the three-dimensional structures of three members of the major facilitator superfamily, the oxalate transporter OxIT from *Oxalobacter formigenes* (Hirai et al., 2002), the lactose permease LacY *Escherichia coli* (Abramson et al., 2003), and the glycerol-3-phosphate transporter GlpT from *Escherichia coli* (Huang et al., 2003) have been reported. These transporters had similar structures containing large clefts that were crystallized in an orientation directed to the cytosol. For LacY it was shown that this cleft contained the substrate binding site. On the basis of the structure of LacY we modelled the

presumed TMHs of rOCT1 with a large cleft similar to LacY. The validity of this model was supported by mutagenesis. Seven amino acids whose mutations increased substrate affinities are located in one region surrounding the large cleft and are accessible from the aqueous phase.

Experimental Procedures

Site-Directed Mutagenesis. Point mutations were introduced in rOCT1 (Gründemann et al., 1994) by polymerase chain reaction (PCR) applying the overlap extension method (Ho et al., 1989). The oligonucleotides used as flanking primers were: 5'CCA TCT ATG TGG GCA TCG3' (rOCT1, nucleotides 138-155) and 5'ACA GCA GGA AGA GGA AGG3' (rOCT1, nucleotides 872-855). The PCR amplicates were digested with *AccI* and *NheI* and gel-purified fragments were ligated into wild-type rOCT1/pRSSP vector (Busch et al., 1996) that was cut with the same restriction endonucleases. The fragments introduced into rOCT1/pRSSP were sequenced to confirm the presence of the desired mutations and to exclude PCR errors. For immunodetection, the FLAG epitope (DYKDDDDK) was added to the C-terminus of rOCT1 wild-type and mutants, employing the overlap extension PCR procedure and using the rOCT1-FLAG primers (with underlined FLAG sequence) 5'GAC TAC AAG GAT GAC GAT GAC AAG TGA CAG GGA TGC TG3' (forward) and 5'CTT GTC ATC GTC ATC CTT GTA GTC AGT ACT TGA GGA CTT G3' (reverse). The PCR amplicates were digested with *Eco130I* and *BgIII*, gel-purified and substituted for the respective fragment of rOCT1 in the rOCT1/pRSSP vector.

cRNA Transcription and Expression in *Xenopus* Oocytes. For injection into *Xenopus* oocytes, m7G(5')ppp(5')G-capped sense cRNAs were transcribed *in vitro* using the "mMESSAGE mMACHINE" kit (Ambion, Cambridgeshire, UK). The pRSSP vectors

containing rOCT1 wild-type or rOCT1 mutants (Busch et al., 1996) were linearized with *Mlu*I, and cRNAs were synthesized using SP6 RNA polymerase. cRNA concentrations were estimated from ethidium bromide-stained agarose gels using polynucleotide marker as standards (Gründemann and Koepsell, 1994). Stage V-VI oocytes were defolliculated with collagenase A (Veyhl et al., 1993) and stored for several hours in Ori buffer [5 mM 3-(*N*-morpholino)propanesulfonic acid-NaOH, pH 7.4, 100 mM NaCl, 3 mM KCl, 2 mM CaCl₂, and 1 mM MgCl₂] supplemented with 50 mg/l gentamicin. The oocytes were injected with 10 ng of the respective cRNA in 50 nl H₂O. For comparison in parallel experiments, cRNAs of wild-type and mutant rOCT1 were injected within 3 h into oocytes from the same batch. For transporter expression, the oocytes were incubated for 3-5 days at 16°C in Ori buffer supplemented with 50 mg/l gentamicin.

Enrichment of Plasma Membranes of *Xenopus* Oocytes. – Three days after incubation of cRNA-injected oocytes or noninjected oocytes in Ori buffer, a plasma membrane-enriched fraction was prepared at 4°C as described (Geering et al., 1989). Oocytes were homogenized in homogenization buffer (10 mM HEPES pH 7.9, 83 mM NaCl, 1 mM MgCl₂, 1 mM PMSF, 0.05 ng/ml leupeptin, 10 mM benzamide), centrifuged for 10 min at 1,000xg and the supernatant was carefully removed leaving lipids behind. The pellet was suspended in homogenization buffer, centrifuged for 10 min at 1,000xg and the supernatant was collected. Both supernatants were combined and centrifuged for 20 min at 10,000xg. The pellet was suspended in homogenization buffer and re-centrifuged for 20 min at 10,000xg. The obtained pellet is enriched in plasma membranes as previously demonstrated by marker enzymes (Geering et al., 1989) and by immunodetection of the expressed Na⁺-D-glucose cotransporter SGLT1 (Valentin et al., 2000). Protein was quantified according to Bradford using bovine serum albumin as standard (Bradford, 1976).

Western blotting. Enriched plasma membrane fractions from *Xenopus* oocytes were incubated for 30 min at 37°C in 60 mM Tris HCl, pH 6.8, 100 mM dithiothreitol, 2% (w/v) SDS, and 7% (v/v) glycerol and separated by SDS-polyacrylamide gel electrophoresis as described (Valentin et al., 2000). Proteins were transferred to polyvinylidene difluoride membrane and incubated with affinity purified polyclonal antibody raised against the large extracellular loop of rOCT1 as described earlier (Meyer-Wentrup et al., 1998). Bound peroxidase-conjugated secondary antibody (goat anti rabbit IgG) was visualized by enhanced chemiluminescence (ECL system; Amersham Buchler, Braunschweig, Germany). Prestained molecular weight marker BenchMark (Life Technologies, Karlsruhe, Germany) was used to determine apparent molecular masses.

Immunocytochemistry. Oocytes were treated as described (Wolff et al., 2001). On day 3 after injection, oocytes were incubated for 5 min in 200 mM K⁺ aspartate, manually devitellinized, and then fixed overnight at -20°C in 80% (v/v) methanol, 20% (v/v) DMSO. The permeabilized oocytes were re-hydrated, washed in phosphate buffered saline (PBS) and incubated at 4°C for 12 h with mouse anti-FLAG M2 IgG monoclonal antibody (Sigma, Deisenhofen, Germany) (dilution 1:2,000) in the presence of 10% (v/v) goat serum (Sigma). After washing in PBS, oocytes were incubated for 1 h at room temperature with secondary Alexa 546 goat anti-mouse IgG antibody (Molecular Probes, Eugene, USA) (dilution 1:200). Oocytes were washed in PBS, postfixed for 30 min at room temperature in 3.7% (v/v) paraformaldehyde, and embedded in acrylamide (Technovit 7100, Heraeus Kulzer, Wehrheim, Germany). Embedded oocytes were cut into 5- μ m sections and analyzed by epifluorescence microscopy.

Tracer Uptake Measurements. For uptake measurements, the oocytes were incubated at 19°C for 30 min in Ori buffer containing [¹⁴C]TEA, [³H]MPP, [¹⁴C]guanidine, [³H]histamine or [³H]serotonin. Oocytes were then added to ice-cold Ori buffer plus 100 μ M quinine, washed in the same buffer, solubilized in 5% (w/v) SDS, and analyzed for radioacti-

vity. Uptake in oocytes expressing rOCT1 wild-type or mutants was corrected for uptake by noninjected oocytes. TEA and MPP uptake by noninjected oocytes was identical to the uptake by oocytes expressing transporter in the presence of 100 μM quinine, an inhibitor of OCTs.

Calculation and statistics. Uptake in oocytes expressing rOCT1 wild-type or mutants was calculated from 7-10 oocytes and corrected for nonspecific uptake measured in 7-10 noninjected control oocytes. K_M and V_{\max} were calculated by fitting the Michaelis-Menten equation to the corrected uptake measured with 7-10 different substrate concentrations. IC_{50} values were calculated from individual experiments by fitting the Hill equation for multisite inhibition to uptake rates in the presence of 7-10 different inhibitor concentrations. Considering the large variations of expression levels and regulatory state between different batches of oocytes, uptake by rOCT1 mutants was always measured in parallel with uptake by rOCT1 wild-type in oocytes from the same batch and within 3 h. The experiments reported in the present paper were performed during a period of 3 years. During this time considerable variability of expressed uptake rates and some variability of the K_M values of individual transporters were observed. For example, for TEA uptake by rOCT1 wild-type, the V_{\max} values varied between 60 and 420 $\text{pmol} \times \text{oocyte}^{-1} \times \text{h}^{-1}$ whereas the K_M values varied between 55 and 133 μM . The large differences in V_{\max} values can be explained by differences in expression level between oocytes batches. The observed differences in K_M values are supposed to be due to oocyte-batch dependent differences in membrane potential or transporter regulation (Mehrens et al., 2000; Arndt et al., 2001). To enable a comparison of mutants, we expressed uptake, K_M , V_{\max} , and IC_{50} as percentages of the respective values for rOCT1 wild-type obtained in parallel measurements. Data are presented as mean \pm SEM values, obtained from 3-6 independent experiments. The paired two-sided Student's *t*-test was used to assess the statistical significance of differences between (*i*) uptake rates of TEA or MPP by mutants vs. wild-type measured in parallel

(Table 1), (ii) relative uptake rates of TEA vs. MPP by individual mutants in parallel experiments (Table 1), (iii) K_M or V_{max} values for mutants vs. wild-type rOCT1 from parallel measurements (Table 2, Fig. 4). Unpaired two-sided Student's *t*-test was employed (i) to compare K_M or V_{max} values for TEA vs. MPP of individual mutants that were obtained from measurements that were not strictly performed in parallel (Fig. 4) or (ii) to compare K_M or V_{max} between different mutants from measurements that were not strictly performed in parallel (Fig.4). In the experimental series shown in Fig. 3 we performed analysis of ANOVA followed by Tukey's test to assess the differences between relative uptake rates of five different substrates by various mutants.

Modelling the Tertiary Structure of rOCT1. We used the tertiary structure of lactose permease LacY from *E. coli* which was recently crystallized (pdb entry 1PV6, Abramson et al., 2003), to model the tertiary structure of the putative transmembrane α -helices (TMHs) of rOCT1. The putative TMHs of rOCT1 indicated in Fig. 6 were predicted using the software TMHMM (<http://www.cbs.dtu.dk/services/TMHMM/>). The putative TMHs of rOCT1 were then aligned to the respective helices of LacY using CLUSTALW or Bestfit of the software package GCG Wisconsin (Accelrys). The model was built by replacing the residues of LacY with the corresponding residues of rOCT1 using the software package Quanta2000 (Accelrys). Close contacts were removed by rotamer searches for the affected side chains. Further steric clashes were eliminated employing energy minimization procedures utilizing the CHARMM forcefield (Accelrys). The backbone geometry was retained by defining distance restraints for the backbone atoms mimicking the hydrogen bonding pattern of LacY. These distance restraints obeyed an NOE-like constraints potential with upper and lower distance boundaries; target distance was set to 2.1Å, lower boundary was set to 1.9Å between the amide proton and the carbonyl oxygen, upper boundary for this atom pair was set to 2.4Å. At sites where non-glycine or non-prolines residues of the LacY template were exchanged to glycine or prolines of rOCT1, no

distance restraints were used to allow for an adaptation of the backbone conformation. The distances were weighted with a rather high force constant of $250 \text{ kcal mol}^{-1} \text{ \AA}^{-2}$ in the initial refinement steps (first 100 minimization steps) and the force constant was then gradually lowered (100 minimization steps per round, lowering the force constant by $50 \text{ kcal mol}^{-1} \text{ \AA}^{-2}$ each round, final force constant $50 \text{ kcal mol}^{-1} \text{ \AA}^{-2}$) to allow for more conformational freedom during the final steps of energy minimization within CHARMM. The overall fold was maintained also by a set of distance restraints that were defined between the N- and C-terminal “ends” of the TMHs. These distance were also used with upper and lower boundaries, however the boundaries were set to $\pm 25\%$ of the respective distance to allow for smaller changes in the packing of the TMHs. After several rounds of energy minimization a short molecular dynamic simulation *in vacuo* (10 ps) was performed with the backbone and overall geometry restrained as indicated above using the CHARM forcefield of the software package QUANTA2000. These maneuvers led to low energies for geometry and van der Waals interaction terms. The large loops of rOCT1 were excluded from the modelling since LacY lacks a corresponding structure (loop between TMH 1 and 2) or exhibits low structural similarity (loop between TMH 6 and 7).

Materials. [^{14}C]tetraethylammonium (TEA) (1.9 TBq/mmol), [^3H]1-methyl-4-phenylpyridinium (MPP) (3.1 TBq/mmol) and [^{14}C]guanidine (2.0 GBq/mmol) were obtained from Biotrend (Köln, Germany). [^3H]histamine (1.9 TBq/mmol) and [^3H]serotonin (0.7 TBq/mmol) were purchased from Amersham Bioscience Europe GmbH (Freiburg, Germany), and tetrapentylammonium (TPeA) from Sigma-Aldrich Chemie GmbH (Taufkirchen, Germany). The other chemicals were obtained as described earlier (Arndt et al., 2001; Meyer-Wentrup et al., 1998).

Results

Mutation Scanning of Amino Acids Comprising the Presumed 4th Transmembrane α -Helix of rOCT1. To investigate the role of the presumed 4th transmembrane α -helix (TMH) for cation selectivity of rOCT1 we replaced each amino acid between positions 212-229 with similar amino acids or with amino acids from corresponding positions in other members of the *SLC22* transporter family (Koepsell et al., 1999). We expressed the mutants in oocytes and measured the uptake rates of 10 μ M [¹⁴C]TEA and of 0.1 μ M [³H]MPP in comparison to wild-type (Table 1). No significant uptake of TEA and MPP was expressed by the mutants K215Q, K215R, E227Q, E227D, and V229L. When V229 was replaced by alanine, a less bulky amino acid than leucine, relatively high uptake rates of TEA (32% of wild-type) and MPP (54% of wild-type) were expressed.

To investigate translation and membrane insertion for mutants that did not express uptake of TEA (K215R, E227D, V229L), we performed Western blots with enriched plasma membranes and investigated the localization of the transporters in intact oocytes. To enable the immunocytochemical detection in acrylamide-embedded oocytes, we appended a FLAG-tag to the C-terminus of wild-type and mutant transporters. With FLAG-tagged wild-type rOCT1, a similar uptake rate of 10 μ M [¹⁴C] TEA was expressed compared to non-modified wild-type. No significant uptake of TEA was expressed with the FLAG-tagged mutants K215R, E227D and V229L as observed with the unmodified mutants (data not shown). Western blots with preparations of enriched plasma membranes obtained by differential centrifugation revealed similar staining for FLAG-tagged wild-type and mutants. The Western blot in Fig.1a was developed with a previously described affinity-purified antibody against the large extracellular loop of rOCT1 (Meyer-Wentrup et al., 1998). The antibody reacted with two polypeptide bands with apparent molecular masses of \sim 50 and \sim 70 kDa and showed a less intense reaction with a \sim 45 kDa protein. The intensity of this band varied between different experiments (Gorboulev et al., 1999).

The upper band was absent after deglycosylation (unpublished data). Together, these data indicate that the mutants are translated and glycosylated similar to rOCT1 wild-type.

Fig. 1b shows immunostaining of oocytes expressing FLAG-tagged wild-type and FLAG-tagged mutants K215R, E227D and V229L using a monoclonal antibody against the FLAG epitope. Immunostaining at the plasma membrane in oocytes expressing rOCT1 wild-type and the mutants indicates translation and membrane insertion. By fluorescence microscopy and confocal laser scanning microscopy we were not able to differentiate staining at the plasma membrane from vesicles just beneath it (data not shown). For this reason and because the FLAG-tag was attached to the intracellular C-termini, the immunolocalization data do not exclude location in vesicles beneath the plasma membrane.

After replacing G216 by alanine, W218 by phenylalanine, S220 by isoleucine, or T226 by alanine, the uptake of 10 μM TEA was reduced to a greater extent than the uptake of 0.1 μM [^3H]MPP (Table 1, $P < 0.05$ for difference). This indicates changes in substrate selectivity². Trends towards altered substrate selectivity were observed for the mutants V213G, Y222F, L224V, and V229A (Table 1). To confirm these trends, and to determine whether the different changes in transport rates of TEA vs. MPP are due to altered affinities or maximal transport velocities, concentration dependence of TEA and MPP uptake was measured (Table 2). In the mutant V213G, the K_M values for both, TEA and MPP were increased significantly compared to wild-type, indicating a decrease in substrate affinity. The increase in K_M value for TEA was significantly higher than the increase in K_M value for MPP. This explains the higher transport activity for MPP vs. TEA measured in Table 1. After mutating G216 to alanine, the K_M values for TEA and MPP were not changed whereas the V_{max} values for both substrates were reduced. The V_{max} for TEA appeared to be reduced to a greater extent than the V_{max} for MPP. This may explain the higher uptake of MPP vs. TEA in Table 1. After replacing W218 by phenylalanine, the V_{max} for TEA was halved whereas the V_{max} for MPP was not changed ($P < 0.05$ for different

effects on V_{\max}). Substrate concentration dependence of mutant S220I revealed a statistically significant reduction of the V_{\max} for TEA and a trend towards a less pronounced reduction of V_{\max} for MPP. This can explain the lower uptake of TEA vs. MPP in Table 1. In mutant Y222F, the K_M for TEA was significantly lower compared to wild-type ($P < 0.05$) whereas the K_M for MPP was not changed. In addition, the V_{\max} values for TEA and MPP were decreased. Since the data indicate an increase in affinity for TEA which may be considered as gain of function, we investigated mutant Y222F in more detail and exchanged Y222 by two other amino acids (see below). After mutation of L224 to valine, the V_{\max} values for TEA and MPP were significantly decreased and a trend for a decrease in K_M values was observed. After exchange of T226 by alanine, the K_M and V_{\max} for MPP were significantly decreased whereas the K_M and V_{\max} for TEA showed only a trend for a decrease. Since also this mutation lead to an affinity increase it was further characterized (see below). Finally, in the V229A mutant, the K_M for TEA was significantly increased vs. wild-type whereas the K_M for MPP was not changed significantly.

Further Characterization of Mutants of Conserved Amino Acids Localized on one Side of the Presumed 4th TMH. Secondary structure prediction suggests a TMH between amino acids 212 and 229 (Koepsell et al., 1999). An α -helical wheel representation of that TMH shows that the two mutations with significantly increased substrate affinity (Y222F, T226A) affect amino acids on the same side of this α -helix (Fig. 2). They belong to a group of five neighbouring amino acids on this side of the presumed 4th TMH (K215, W218, Y222, T226, V229) that are conserved in organic cation transporters but not in organic anion transporters (Koepsell et al., 1999). We further characterized the function of these amino acids by additional transport measurements and in additional mutations (W218Y, W218L, Y222L). To identify putative changes in substrate selectivity in point mutation, we measured the uptake of 10 μM [^{14}C]TEA, 0.5 μM [^3H]MPP, 200 μM [^{14}C]guanidine, 30 μM [^3H]histamine, or 2.5 μM [^3H]serotonin in

the mutants K215Q, K215R, W218F, W218Y, W218L, Y222F, Y222L, T226A, V229L, and V229A in comparison to rOCT1 wild-type. Note that the substrate concentrations employed in these experiments were more than $8 \times$ lower than the respective K_M values in rOCT1 wild-type (Arndt et al., 2001; Koepsell et al., 2003); therefore, changes in the uptake rates may reflect changes in affinity, maximal transport velocity, or both.

Mutants K215Q, K215R, and V229L which did not mediate uptake of TEA and MPP (see Table 1) were also not able to mediate uptake of guanidine, histamine or serotonin (data not shown). With mutant V229A, uptake rates for TEA, MPP, guanidine, histamine, and serotonin were about 50% of the respective uptake rates observed with rOCT1 wild-type. The substrate selectivity of this mutant was not different from wild-type (data not shown). Mutants W218F, W218Y and W218L exhibit significantly different substrate selectivities between each other and compared to rOCT1 wild-type (Fig. 3). In all three W218 mutants, the smallest changes of uptake rates compared to wild-type were observed for MPP. In W218F and W218Y, the uptake rates for MPP were similar to wild-type, but reduced by about 80% in W218L. Significant changes in substrate selectivity were also observed after mutations of Y222 and T226 (Fig. 3). Substrate selectivity was changed in mutant Y222L but not in Y222F. A unique substrate selectivity different from wild-type was also obtained in the T226A mutant.

When changes in substrate selectivity are identified by uptake measurements of different substrates using a single fixed concentration of each substrate as in Fig. 3, changes in affinity cannot be distinguished from changes of maximal transport rate. Changes in K_M may thus be overlooked if they are combined with opposite changes of V_{max} . For example, after replacement of Y222 by phenylalanine, the uptake rates of 10 μ M TEA and 0.5 μ M MPP were similar to wild-type (Fig. 3) although the K_M and V_{max} values for TEA were significantly decreased compared to wild-type (Table 2). When the affinity of a substrate is increased after a point mutation, we reasoned that the respective amino

acid may be involved in substrate binding because it is not very likely that an increase of affinity is caused by an indirect effect on the structure. It is obvious that point mutations in a substrate binding site can lead to a decrease in substrate affinity, however, there is a high probability that mutations outside a binding site induce structural changes that have the same effect.

A significant decrease of the K_M for TEA was observed in mutant Y222F, and a significant decrease of the K_M for MPP in mutant T226A (Table 2). Thus, Y222 and T226 are probably localized in the substrate binding region of rOCT1. To understand the functional role of W218 which is localized next to Y222 on the α -helix, and to further investigate the functional role of Y222, we compared substrate dependence of TEA uptake vs. MPP uptake after replacement of W218 by phenylalanine, tyrosine and leucine, and after replacement of Y222 by phenylalanine and leucine. Fig. 4 shows the apparent K_M and V_{max} values of these mutants. As described above, the K_M values for TEA and MPP and the V_{MAX} for MPP were not changed by the W218F mutation whereas the V_{max} for TEA uptake was decreased by 50% (Table 2 and Fig. 4). When W218 was replaced by tyrosine, the function of rOCT1 was changed in a different way: K_M and V_{max} values for both, TEA and MPP, were decreased significantly compared to wild-type. Note, that the additional hydroxyl group in W218Y compared to W218F leads to a higher affinity for both, MPP and TEA. Replacement of W218 by leucine resulted in a drastic decrease of the affinity for TEA whereas the affinity for MPP was not changed. At variance, after the exchange of this amino acid, the V_{max} values for TEA and MPP uptake were decreased by similar degrees. In summary, point mutations in position 218 can lead to changes in substrate affinity and transport rates that are independent from each other. The changes in substrate affinity can be specific for certain substrates and can include an increase of substrate affinity. The data suggest that in addition to Y222 and T226, also W218 is localized within the substrate binding region of rOCT1 and that W218 can interact with both TEA and MPP. The K_M

independent changes of V_{\max} observed in mutants W218F and W218L suggest that W218 participates in conformational changes during substrate translocation.

Different effects on the affinity of TEA and MPP were also observed when Y222 was replaced by phenylalanine or leucine. As described above, the K_M for TEA uptake in Y222F was significantly decreased, whereas the K_M for MPP uptake remained unchanged suggesting that Y222 is located in the substrate binding region (Table 2, Fig.4). When Y222 was replaced by leucine, the K_M for TEA and MPP decreased by similar degrees (Fig. 4, TEA by 53%, MPP by 65%). In parallel, the V_{\max} values for TEA and MPP were decreased by 91 and 90%, respectively. The functional properties of Y222L support the interpretation that Y222 is localized in the substrate region of rOCT1.

To further characterize mutants Y222F and Y222L we investigated the effect of these mutations on two high affinity inhibitors, cyanine863, and the quaternary ammonium salt tetrapentylammonium (TPeA). Previous mutagenesis showed that TPeA binds to the substrate binding region of rOCT1 (Gorboulev et al., 1999). In the Y222F mutant, the IC_{50} value for inhibition of TEA (10 μ M) uptake by cyanine863 was not significantly different from rOCT1 wild-type (data not shown). However, the IC_{50} value for inhibition of TEA uptake by TPeA was largely decreased (Fig. 5). For inhibition of TEA uptake by TPeA we determined IC_{50} values (mean \pm SEM, n=3) of 1.0 ± 0.2 μ M (rOCT1 wild-type, Hill coefficient 0.58 ± 0.05) and 0.05 ± 0.02 μ M (Y222F, Hill coefficient 0.66 ± 0.10) ($P < 0.05$ for difference of IC_{50} values). The IC_{50} for TPeA inhibition of TEA uptake by the Y222L mutant was not significantly different from wild-type ($IC_{50} = 2.2 \pm 0.7$, n=3, Hill coefficient 1.0 ± 0.1). Taken together, the data confirm the interpretation that Y222 is located within the substrate binding region of rOCT1 and suggest that Y222 interacts with TEA, MPP and TPeA .

In this study, we estimated the affinity of rOCT1 wild-type and mutants for TEA and MPP by calculating apparent K_M values from substrate concentration dependence of

uptake. Experiments in the accompanying paper showed that the K_M values for TEA or MPP uptake by rOCT1 wild-type and two rOCT1 mutants with increased substrate affinity (rOCT1 L447Y/Q448E, rOCT1 A443I/L447Y/Q448E) were not significantly different from the IC_{50} values for inhibition of MPP (0.1 μ M) uptake by TEA, or for the inhibition of TEA (10 μ M) uptake by MPP (Gorboulev et al., 2005). In the present paper we compared K_M and IC_{50} values of additional mutants. We expressed the mutants W218F, W218Y, W218L in parallel with rOCT1 wild-type and measured both, the apparent K_M values for substrate activation of TEA uptake and the IC_{50} values for inhibition of MPP (0.1 μ M) uptake by TEA. From three independent experiments, the following K_M vs. IC_{50} values were determined: rOCT1 wild-type 94 ± 27 vs. 122 ± 20 μ M, W218F 41 ± 6 vs. 69 ± 23 μ M, W218Y 30 ± 5 vs. 38 ± 6 μ M, and W218L 760 ± 149 vs. 854 ± 90 μ M. The Hill coefficients calculated from the inhibition experiments were not significantly different (rOCT1 wild-type 0.92 ± 0.13 , W218F 0.72 ± 0.14 , W218Y 0.72 ± 0.05 , and W218L 1.07 ± 0.18). In conclusion, the comparisons between K_M vs. IC_{50} values for TEA and MPP performed so far suggest that the same binding steps of TEA and MPP are characterized by both methods.

Modelling the Structure of the Substrate Binding Pocket of rOCT1. Recently the lactose permease LacY of *Escherichia coli* was crystallized and the tertiary structure determined at 3.3 Å resolution (Abramson et al., 2003). Since LacY and the organic cation transporters belong to the major facilitator superfamily (MFS) we tried to model the tertiary structure of the presumed transmembrane α -helices of rOCT1 on the basis of the LacY structure. To test the validity of the structural model we analyzed whether the amino acids that have been located within the substrate binding site by mutagenesis experiments, line the substrate binding pocket predicted by the model. By mutagenesis experiments three amino acids on one side of the 4th TMD (W218, Y222, T226, see above), three amino acids in the 10th TMD (A443, L447, Q448, (Gorboulev et al., 2005)), and one amino acid

in the 11th TMD (D475, Gorboulev et al., 1999) were assigned to the substrate binding region of rOCT1. Fig. 6 shows an alignment of the presumed TMHs of the three OCT subtypes from rat and human with the respective helices of the LacY. For the sequences shown in Fig. 6, 12.4% of the amino acids were identical between rOCT1 and LacY whereas 28.8% of the amino acids were similar. Considering the sequences of the three OCT subtypes from human and rat together, 18.5% of amino acids were identical and 37% of the amino acids were similar between at least one of the OCTs and LacY. By analogy to the tertiary structure of LacY (Abramson et al., 2003) and two other transporters of the MFS superfamily, the oxalate transporter OxIT from *Oxalalobacter formigenes* (Hirai et al., 2002) and the glycerol-3-phosphate transporter GlpT from *E. coli*. (Huang et al., 2003), the model in Fig. 7 shows a large cleft in rOCT1 that is accessible from the intracellular side of the membrane. The cleft in rOCT1 is formed by the 1st, 2nd, 4th, 5th, 7th, 8th, 10th and 11th TMH (Fig. 7a). The model is strongly supported by our mutagenesis experiments because all amino acids that have been identified to be involved in the substrate binding (4th TMH W218, Y222 and T226, 10th TMH A443, L447 and Q448, 11th TMH D475) are located in the large cleft of the modelled transporter and are accessible from the aqueous phase (Fig.7a-c). Note that these amino acids are located at a similar depth within the large cleft. They may be part of a substrate binding region surrounding the cleft. The cross-area of the cleft in this part is about 20Å × 60 Å. The cleft has a depth of about 80 Å. The comparison of the modelled substrate binding region surrounding the cleft with the sizes of TEA, MPP and corticosterone suggests that more than one of these compounds can bind at the same time.

Since similar high resolution tertiary structures have been reported for LacY and GlpT (Abramson et al., 2003; Huang et al., 2003) and the amino acid similarity between these transporters is not larger than the similarity between rOCT1 and LacY, it is likely that the tertiary structure of rOCT1 is similar to both proteins. A comparison between the

structures of LacY and GlpT showed that the transmembrane topology is highly conserved between these two transporters, a structural alignment yields a root mean square deviation of 4Å if the C α atoms of 382 equivalent residues are considered (PDB entry 1PW4 was used for GlpT, PDB entry 1PV6 was used for LacY). Comparing the structural model of rOCT1 with to tertiary structure of GlpT, the C α atoms of the seven residues within the substrate binding region of rOCT1 are within a distance of less than 4Å compared to the respective residues of GlpT and exhibit similar side chain orientations.

Discussion

The mutagenesis experiments presented in this paper strongly suggest that the three amino acids W218, Y222, and T226 on succeeding turns of the presumed 4th TMH form part of the substrate binding region of rOCT1. Mutations in these amino acids resulted in significant decreases of K_M values for MPP and/or TEA. In mutants W218Y and Y222L the K_M values were decreased for both TEA and MPP, in mutant Y222F the K_M value for TEA was decreased, and in mutant T226 the K_M value for MPP was decreased. The data suggest that TEA and MPP bind to W218 and Y222 and that MPP binds also to T226. Ionic interaction of the positive charges in TEA and MPP with π -electrons of W218 and Y222 (Dougherty, 1996) as well as hydrophobic and van der Waals interactions with W218, Y222 and T226 may be involved. W218 is supposed to play a role in TEA translocation because in the W218F mutant the V_{max} value for TEA was decreased whereas the K_M for TEA remained unchanged. Y222 may be important for the translocation of MPP since in the Y222F mutant the V_{max} value for MPP was decreased whereas the K_M for MPP was not altered.

Mutation of other amino acids in the presumed 4th TMH drastically decreased transport activity (K215Q, K215R, E227Q, E227D, V229L, see Table 1) or increased K_M

value for TEA and changed substrate selectivity (V213G, V229A, see Table 2). These amino acids may be crucial for the tertiary structure of the substrate binding region. In mutant V213G, the K_M values for TEA and MPP were increased by different degrees, and in mutant V229A, the K_M value for TEA was increased whereas the K_M value for MPP was not changed. V213 is localized on the opposite side of the presumed 4th TMH compared to W218, Y222 and T226 (see Fig. 2). Its replacement by alanine may change the position of the 4th TMH and thus the position of W218, Y222 and T226 (see model in Fig. 7a,c). V229 on the same side of the 4th TMH as W218, Y222 and T226 (Fig. 2) is located close to the transition between the 4th and 5th TMH (Fig 7c). After replacement of V229 by leucine, this more bulky amino acid compared to valine or alanine may interact with the 5th TMH and thereby change the position of 4th TMH that contains the above described substrate binding domain.

The crystal structure of the lactose permease LacY from *E. coli* (Abramson et al., 2003) provided the possibility to model the tertiary structure of the TMHs of rOCT1. rOCT1 belongs to the same MFS superfamily of transporters as LacY (Koepsell et al., 2003), and shows 29% similar amino acids in the TMHs. We tested the validity of the structural rOCT1 model by evaluating the localization of seven amino acids that have been shown to be involved in substrate binding by mutagenesis experiments. Three amino acids on the presumed 4th TMH (W218, Y222, T226) were identified above, three amino acids on the presumed 10th TMH (A443, L447, Q448) were identified in the accompanying paper (Gorboulev et al., 2005), and one amino acid in the 11th TMH (D475) was identified earlier (Gorboulev et al., 1999). All seven amino acids fulfill the criterium that their exchange with an appropriate amino acid lead to an increase of substrate affinity that was often combined with a change in substrate selectivity. Such a change of function is not likely to be induced by indirect effects. For W218, Y222 and T226, indirect effects can be virtually excluded as reason for the observed affinity changes in all three positions. The high quality

of our model of rOCT1 is strongly supported by the finding that all seven amino acids, which belong to the substrate binding region as judged from mutagenesis, are located within one structural epitope in the large cleft of the rOCT1 model and are in contact with the aqueous phase.

The positions of the seven amino acids in the modelled cleft of rOCT1 suggests that two or more substrates can bind in parallel to this conformation of the transporter. A decrease of the K_M value for TEA was observed after mutations of D475 in the 11th TMH (Gorboulev et al., 1999), of W218 or Y222 on successive turns of the 4th TMH, and after a combined mutation of A443, L447 and Q448 in the 10th TMH (Gorboulev et al., 2005), and in our model one TEA molecule cannot interact simultaneously with D475, W218, Y222, and an amino acid in the 10th TMH. Our mutagenesis experiments indicate that the binding sites for TEA in the proposed substrate binding region overlap with the binding sites for MPP, TPcA and/or corticosterone. Note that in addition to TEA (*i*) the affinity for MPP was increased in mutants of W218, of Y222 and in the triple mutant A443/L447/Q448, (*ii*) the affinity of corticosterone was increased after mutations of A443, L447 and /or Q448, and (*iii*) the affinity for TPcA was increased after mutations of D475 and Y222 (see above, Gorboulev et al., 1999, and Gorboulev et al., 2005).

Our interpretation that two or more substrates and/or inhibitors can bind at the same time is supported by data that suggest short-range allosteric interactions between ligands within the substrate binding region of rOCT1 (Gorboulev et al., 2005). After exchanging two amino acids in the substrate binding region (L447Y/Q448E) we observed a significantly higher affinity for inhibition of TEA (10 μ M) uptake by corticosterone compared to the inhibition of MPP (0.1 μ M) uptake by corticosterone. These data suggest different short-range allosteric interactions between TEA and corticosterone vs. MPP and corticosterone because (*i*) TEA, MPP and corticosterone bind to the substrate binding region, (*ii*) the differences in corticosterone affinity cannot be explained with different

replacement of corticosterone by the two substrates, and (iii) it is unlikely that the observed substrate effect on corticosterone affinity is due to allosteric interaction between rOCT1 monomers because it was only observed after mutation of two amino acids in the substrate binding region.

The question arises whether simultaneous binding of more than one substrate molecule to the substrate binding region of rOCT1 is compatible with the observations (i) that rOCT1 exhibits Michaelis-Menten type kinetics (Koepsell et al., 2003), (ii) that the IC_{50} values measured for TEA inhibition of MPP (0.1 μ M) uptake expressed by rOCT1 and various mutants were similar to the K_M values for TEA (see above), and (iii) that mutations of amino acids at distant locations within the substrate region lead to decreases of K_M and IC_{50} values (see above). These observations could be reconciled if transport of TEA or MPP requires simultaneous or successive substrate binding to two or more binding sites within the large cleft and if the K_M and IC_{50} values reflect binding to more than one of these sites. In addition it is possible that the outwardly directed conformation of the substrate binding region has a more tight structure that allows the simultaneous interaction of one TEA molecule with D475, W218, Y222, and one amino acids in the 10th TMH. Measuring the substrate concentration dependence of cation uptake by rOCT1 wild-type and mutants, so far no sign for cooperativity was detected. At variance, in some cases we obtained Hill coefficients different from 1 for the inhibition of cation uptake (e.g. for inhibition of OCT1 wild-type and Y222F mutant by TPcA, see Fig. 5). Ligand binding measurements with rOCT1 and mutants are required to prove simultaneous ligand binding and short-range allosteric interactions within the binding region. Molecular monitoring of structural changes within the substrate binding region may provide additional insights.

The proposed hypothesis that rOCT1 contains a large substrate binding region within a large cleft that can bind simultaneously several substrates and/or inhibitors is consistent with the crystal structure of the multidrug efflux pump AcrB from *E. coli* (Yu et al., 2003).

AcrB is a polyspecific transporter like rOCT1, however, it has no structural similarity to rOCT1 and is energized by a proton-gradient. Interestingly, crystal structures of AcrB-ligand complexes showed, *(i)* that three ligands bind simultaneously to a binding region of AcrB, *(ii)* that different ligands use a slightly different subset of AcrB residues for binding, and *(iii)* that the bound ligands interact with each other. At variance to AcrB which contains a channel-like transmembrane path, the proposed LacY-like structure of rOCT1 implicates and functional data suggest that the large cleft in rOCT1 may be accessible either from the intracellular side of the plasma membrane or from the extracellular side of the plasma membrane (Volk et al., 2003). It is a challenge to determine the crystal structure of rOCT1 and resolve the transport mechanism.

References

- Abramson J, Smirnova I, Kasho V, Verner G, Kaback HR, and Iwata S (2003) Structure and mechanism of the lactose permease of *Escherichia coli*. *Science* **301**: 610-615.
- Arndt P, Volk C, Gorboulev V, Budiman T, Popp C, Ulzheimer-Teuber I, Akhoundova A, Koppatz S, Bamberg E, Nagel G, and Koepsell H (2001) Interaction of cations, anions, and weak base quinine with rat renal cation transporter rOCT2 compared with rOCT1. *Am J Physiol Renal Physiol* **281**: F454-F468.
- Bradford MM (1976) A rapid and sensitive method for the quantification of microgram quantities of protein utilizing the principle of protein-dye binding. *Anal Biochem* **72**: 248-254.
- Budiman T, Bamberg E, Koepsell H, and Nagel G (2000) Mechanism of electrogenic cation transport by the cloned organic cation transporter 2 from rat. *J Biol Chem* **275**:29413-29420.
- Busch AE, Quester S, Ulzheimer JC, Waldegger S, Gorboulev V, Arndt P, Lang F, and Koepsell H (1996) Electrogenic properties and substrate specificity of the polyspecific rat cation transporter rOCT1. *J Biol Chem* **271**:32599-32604.
- Dougherty DA (1996) Cation- π interactions in chemistry and biology: a new view of benzene, Phe, Tyr, and Trp. *Science* **271**:163-168.
- Geering K, Theulaz I, Verrey F, Häuptle MT, and Rossier BC (1989) A role for the β -subunit in the expression of functional Na⁺-K⁺-ATPase in *Xenopus* oocytes. *Am J Physiol* **257**:C851-C858.

- Gorboulev V, Shatskaya N, Volk C, and Koepsell H (2005) Subtype-specific affinity for corticosterone of rat organic cation transporters 1 and 2 depends on three different amino acids within the substrate binding region. *Mol Pharmacol* (submitted).
- Gorboulev V, Ulzheimer JC, Akhoundova A, Ulzheimer-Teuber I, Karbach U, Quester S, Baumann C, Lang F, Busch AE, and Koepsell H (1997) Cloning and characterization of two human polyspecific organic cation transporters. *DNA Cell Biol* **16**:871-881.
- Gorboulev V, Volk C, Arndt P, Akhoundova A, and Koepsell H (1999) Selectivity of the polyspecific cation transporter rOCT1 is changed by mutation of aspartate 475 to glutamate. *Mol Pharmacol* **56**:1254-1261.
- Gründemann D, Gorboulev V, Gambaryan S, Veyhl M, and Koepsell H (1994) Drug excretion mediated by a new prototype of polyspecific transporter. *Nature* **372**:549-552.
- Gründemann D and Koepsell H (1994) Ethidium bromide staining during denaturation with glyoxal for sensitive detection of RNA in agarose gel electrophoresis. *Anal Biochem* **216**:459-461.
- Hirai T, Heymann JAW, Shi D, Sarker R, Maloney PC, and Subramaniam S (2002) Three-dimensional structure of a bacterial oxalate transporter. *Nat struct biol* **9**:597-600.
- Ho SN, Hunt HD, Horton RM, Pullen JK, and Pease LR (1989) Site-directed mutagenesis by overlap extension using the polymerase chain reaction. *Gene* **77**:51-59.
- Huang Y, Lemieux MJ, Song J, Auer M, and Wang D-N (2003) Structure and mechanism of the glycerol-3-phosphate transporter from *Escherichia coli*. *Science* **301**:616-620.
- Koepsell H (2004) Polyspecific organic cation transporters: their functions and interactions with drugs. *TiPS* **25**:375-381.

- Koepsell H and Endou H (2004) The SLC22 drug transporter family. *Pflugers Arch* **447**:666-676.
- Koepsell H, Gorboulev V, and Arndt P (1999) Molecular pharmacology of organic cation transporters in kidney. *J Membrane Biol* **167**:103-117.
- Koepsell H, Schmitt BM, and Gorboulev V (2003) Organic cation transporters. *Rev Physiol Biochem Pharmacol* **150**:36-90.
- Mehrens T, Lelleck S, Çetinkaya I, Knollmann M, Hohage H, Gorboulev V, Bokník P, Koepsell H, and Schlatter E (2000) The affinity of the organic cation transporter rOCT1 is increased by protein kinase C-dependent phosphorylation. *J Am Soc Nephrol* **11**:1216-1224.
- Meyer-Wentrup F, Karbach U, Gorboulev V, Arndt P, and Koepsell H (1998) Membrane localization of the electrogenic cation transporter rOCT1 in rat liver. *Biochem Biophys Res Commun* **248**:673-678.
- Valentin M, Kühlkamp T, Wagner K, Krohne G, Arndt P, Baumgarten K, Weber W-M, Segal A, Veyhl M, and Koepsell H (2000) The transport modifier RS1 is localized at the inner side of the plasma membrane and changes membrane capacitance. *Biochim Biophys Acta* **1468**:367-380.
- Veyhl M, Spangenberg J, Püschel B, Poppe R, Dekel C, Fritzsich G, Haase W, and Koepsell H (1993) Cloning of a membrane-associated protein which modifies activity and properties of the Na⁺-D-glucose cotransporter. *J Biol Chem* **268**:25041-25053.
- Volk C, Gorboulev V, Budiman T, Nagel G, and Koepsell H (2003) Different affinities of inhibitors to the outwardly and inwardly directed substrate binding site of organic cation transporter 2. *Mol Pharmacol* **64**:1037-1047.

Wolff NA, Grünwald B, Friedrich B, Lang F, Godehardt S, and Burckhardt G (2001)

Cationic amino acids involved in dicarboxylate binding of the flounder renal organic anion transporter. *J Am Soc Nephrol* **12**:2012-2018.

Yu EW, McDermott G, Zgurskaya HI, Nikaido H, and Koshland DE, Jr. (2003) Structural

basis of multiple drug-binding capacity of the AcrB multidrug efflux pump. *Science* **300**:976-980.

Footnotes

This study was supported by the Deutsche Forschungsgemeinschaft Grant SFB 487/A4.

¹C.P and V.G. contributed equally to the work.

²We use the term “change in substrate selectivity” in a broad sense. It means that the relation between uptake rates of two (or more) substrates is changed under at least one experimental condition. Such a “change in substrate selectivity” can show up at low substrate concentrations, at high substrate concentrations, or under both conditions. It may be due to substrate specific changes in turnover (V_{\max}) and/or K_M . Changes in substrate selectivity of mutants relative to wild-type indicate substrate specific changes of uptake rates. Such changes do not necessarily alter the rank order of uptake rates between substrates.

Reprint requests should be addressed to: Hermann Koepsell, Institute of Anatomy and Cell Biology, Koellikerstr. 6, 97070 Würzburg, Germany, E-mail: Hermann@Koepsell.de

LEGENDS TO THE FIGURES

Fig. 1. Demonstration of translation, membrane incorporation and plasma membrane association of inactive mutants. rOCT1 wild-type and the indicated mutants, all tagged with a FLAG-epitope at the C-terminus, were expressed in *Xenopus* oocytes. a) Western blot on plasma membrane enriched subcellular fractions isolated from oocytes injected with water or respective cRNAs. The blots were stained with affinity purified antibody directed against the large extracellular loop of rOCT1. b) Location of expressed rOCT1 wild-type and mutants at the plasma membrane. The oocytes were fixed, permeabilized and stained with an antibody directed against the FLAG-epitope. The data show that mutants K215R, E227D and V229L are translated into protein and transported to the plasma membrane.

Fig. 2. Synopsis of mutational analysis of the presumed 4th TMH of rOCT1 shown as helical wheel. TMH4 is assumed to be a standard α -helix with 3.6 residues/helical turn and each residue is plotted every 100° around the center of the circle starting with M212. *Circles*, amino acids that are conserved in the OCTs but not in the OATs (in mOCT3 and rOCT3 Y222 is replaced by tyrosine). *Box*, E227 is conserved throughout all transporters of the *SLC22* family. (\times), mutants in these positions were inactive. (\circ) mutants in these positions revealed decreased K_M values. (\square) mutants in these positions had increased K_M values. (\bullet) mutants in these positions exhibited changed selectivity. Mutants of the unlabelled amino acids did not show significant changes of functional properties.

Fig. 3. Changes of substrate selectivity after mutation of amino acids on one side of the presumed 4th TMH. Noninjected oocytes, oocytes injected with cRNAs of rOCT1 wild-type, and oocytes injected with cRNAs of mutants were incubated for 3 days. For transport

measurements, the oocytes were incubated for 30 min with 10 μM [^{14}C]TEA, 0.5 μM [^3H]MPP, 0.2 mM [^{14}C]guanidine, 30 μM [^3H]histamine, or 2.5 μM [^3H]serotonin, and the uptake of radioactivity was measured. The uptake by oocytes expressing rOCT1 mutant was corrected for uptake by noninjected oocytes and normalized to the corrected uptake by rOCT1 wild-type measured in parallel. Mean values \pm SEM of 3-4 individual experiments in which the five different substrates were measured in parallel are presented. * $P < 0.05$, ** $P < 0.01$, *** $P < 0.001$, statistical significance of differences between relative uptake rates of different substrates (ANOVA with post-hoc Tukey's test). The indicated rank order of substrates describes the magnitude of changes in transport rates in the mutants compared to wild-type. The data show unaltered substrate selectivity of Y222F and changed substrate selectivities of W218F, W218Y, W218L, Y222L, and T226.

Fig. 4. Concentration dependence of TEA and MPP transport by rOCT1 upon mutation of W218 and Y222. In each experiment, noninjected oocytes, oocytes injected with rOCT1 wild-type cRNA, and oocytes injected with mutant cRNAs were incubated for 3 days, and uptake of [^{14}C]TEA or [^3H]MPP was measured at various concentrations of the respective substrate. Uptake in oocytes expressing rOCT1 wild-type or mutants were corrected for the uptake measured in noninjected oocytes. K_M and V_{\max} values were calculated and normalized to the K_M and V_{\max} values of rOCT1 wild-type measured in the respective experiment. Mean values \pm SEM of 3-4 individual experiments are presented. * $P < 0.05$, ** $P < 0.01$, *** $P < 0.001$, statistical significance of differences between wild-type and mutants. • $P < 0.05$, •• $P < 0.01$, ••• $P < 0.001$, statistical significance for difference of K_M or V_{\max} values between different mutants. * $P < 0.05$, statistical significance of difference of K_M for TEA vs. MPP or of V_{\max} for TEA vs. MPP. The data show that K_M values for TEA and MPP were decreased in parallel or separately when W218 and Y222 were replaced by different amino acids.

Fig. 5 Inhibition of TEA uptake by TPeA in rOCT1 wild-type and mutants Y222F and Y222L. Uptake of 10 μ M [14 C]TEA was measured in the presence of the indicated concentrations of TPeA. A representative experiment of three is shown. The Hill equation was fitted to the data. The IC₅₀ value of TPeA was largely decreased in the Y222F mutant.

Fig. 6 Amino acid alignment of the presumed TMHs of OCTs with the TMHs of LacY from *E. coli*. The three OCT subtypes from rat (rOCT1, rOCT2, rOCT3) and human (hOCT1, hOCT2, hOCT3) were aligned with LacY. Amino acids that are identical between lactose permease and organic cation transporters are indicated in bold face and similar amino acids are shadowed. Numbering is performed according to rOCT1 (Gründemann et al., 1994).

Fig. 7 Structure model of of rOCT1. Modelling was performed using the tertiary structure of LacY (PDB entry 1PV6) from *E. coli*. a, stereo view of a ribbon presentation of the rOCT1 model. The individual TMHs are numbered. The 4th, 10th and 11th TMH are colored in green, blue and red, respectively. Amino acid side chains on these TMHs that have been localized to the substrate binding region by mutagenesis experiments are depicted (W218, Y222 and T226 on the 4th TMH, A443, L447 and Q448 on the 10th TMH, and D475 on the 11th TMH). b, stereo view of the van der Waals surface of the rOCT1 model (cytoplasmic view). In this orientation only four of the above mentioned seven amino acids are visible, however, all seven are located on the accessible surface of the binding region surrounding the cleft. c, ribbon representation of the rOCT1 model oriented as in panel b to show the location of all seven amino acids. The side chains of amino acids W218, Y222, T226, A443, L447, Q448 and D475 are indicated. Numbering of amino acids W218 and A443 is omitted for sake of clarity. d, molecular structures of TEA, MPP and corticosterone in two

magnifications, the presentation of the upper panel shows the size in respect to the model of rOCT1 in panels a to c, the lower panel shows the structures in a larger representation, the size bar is for the lower panel.

TABLE 1

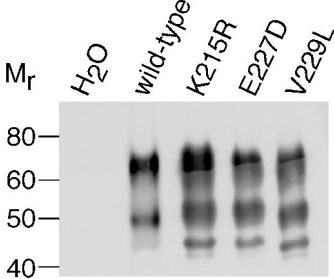
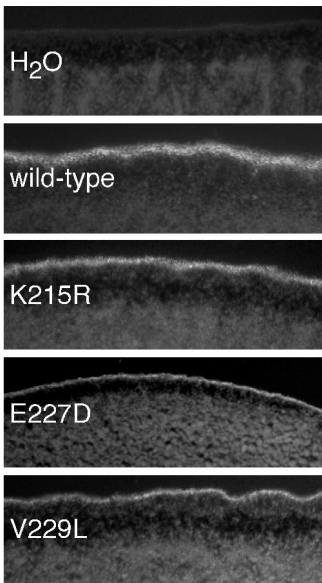
Comparison of uptake rates of TEA and MPP by rOCT1 mutants in which one of the amino acids between positions 212 and 229 was exchanged. rOCT1 wild-type and the indicated mutants of rOCT1 were expressed in oocytes. The uptake of 10 μ M [14 C]TEA or 0.1 μ M [3 H]MPP over 30 min was corrected for non-specific uptake by noninjected oocytes and expressed as percentage of the uptake by rOCT1 wild-type which was measured in parallel. Mean \pm SEM from 3-6 experiments are presented. *P<0.05, **P<0.01, ***P<0.001, statistical significance of differences between wild-type vs. mutants. •P<0.05, statistical significance of difference between TEA vs. MPP in individual mutants. Inactive mutants are indicated by \times .

Mutants	Uptake [% of wild-type]	
	TEA	MPP
M212L	97 \pm 10	98 \pm 7
V213G	28 \pm 9*	51 \pm 12
S214G	42 \pm 1***	44 \pm 12*
\times K215Q	0 \pm 0.1***	0.1 \pm 0.1***
\times K215R	0.2 \pm 0.1***	1.6 \pm 0.5***
G216A	8.7 \pm 1.9*** •	24 \pm 2***
S217G	118 \pm 28	128 \pm 21
W218F	28 \pm 5** •	133 \pm 43
V219L	69 \pm 9	90 \pm 20
S220I	26 \pm 4** •	53 \pm 3*
G221A	42 \pm 9*	57 \pm 9*
Y222F	78 \pm 9	122 \pm 30
T223I	64 \pm 5*	75 \pm 24
L224V	17 \pm 6**	34 \pm 10*
I225G	83 \pm 9	92 \pm 7
T226A	76 \pm 4* •	90 \pm 3
\times E227Q	0.1 \pm 0.1***	0.1 \pm 0.2***
\times E227D	0 \pm 0.1***	0 \pm 0.1***
F228I	89 \pm 10	88 \pm 12
V229A	32 \pm 13*	54 \pm 8*
\times V229L	0.2 \pm 0.1***	0.1 \pm 0.1***

TABLE 2.

K_M and V_{max} for TEA and MPP uptake by rOCT1 mutated at single amino acids within the presumed 4th TMH. Parallel measurements were performed with non-injected oocytes, oocytes expressing rOCT1 wild-type, and oocytes expressing rOCT1 mutants. Uptake rates in oocytes expressing rOCT1 wild-type or mutants were corrected for uptake in noninjected oocytes. The Michaelis Menten equation was fitted to the data of individual experiments. K_M and V_{max} values calculated for mutants are presented as percentages of values that were measured in parallel for rOCT1 wild-type. Mean \pm SEM of three independent experiments are shown. * $P < 0.05$, ** $P < 0.01$, statistical significance of differences between wild-type and mutants. • $P < 0.05$, statistical significance between TEA and MPP uptake.

Mutants	K_M [% of wild-type]		V_{max} [% of wildtype]	
	TEA	MPP	TEA	MPP
V213G	432 \pm 18* •	279 \pm 43*	66 \pm 14	69 \pm 8
G216A	90 \pm 23	158 \pm 62	8 \pm 3**	17 \pm 6**
W218F	81 \pm 13	86 \pm 19	46 \pm 14 •	96 \pm 10
S220I	193 \pm 48	212 \pm 56	41 \pm 10*	67 \pm 10
Y222F	31 \pm 8* •	112 \pm 22	29 \pm 3*	57 \pm 11*
L224V	43 \pm 17	53 \pm 24	10 \pm 4**	16 \pm 3*
T226A	64 \pm 18	33 \pm 4*	48 \pm 8	46 \pm 3**
V229A	313 \pm 68*	137 \pm 34	56 \pm 12	57 \pm 15

a**b****Fig. 1**

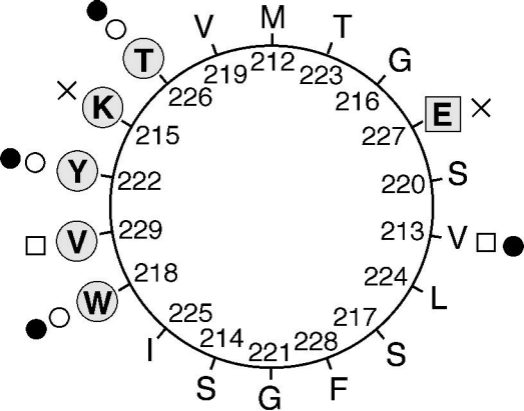


Fig. 2

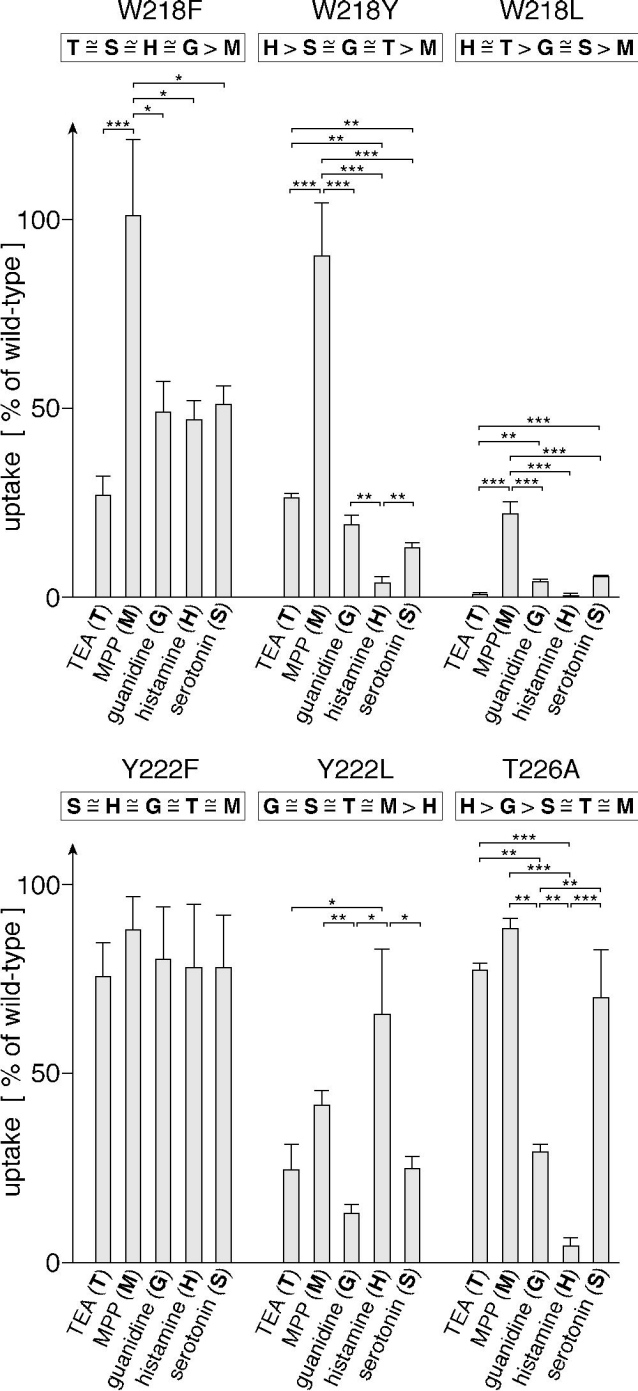


Fig. 3

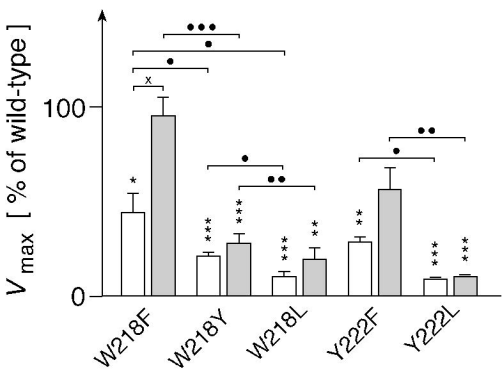
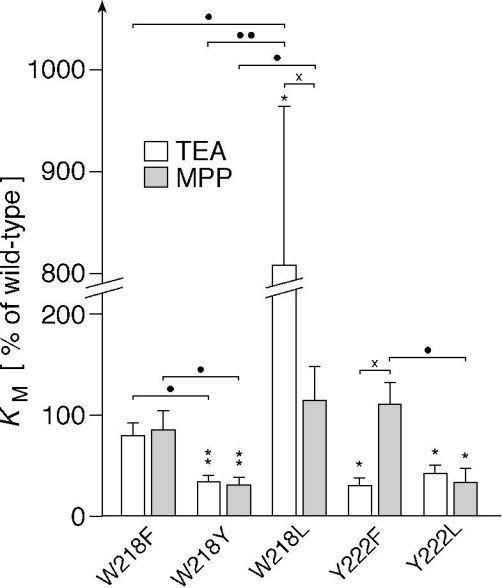


Fig. 4

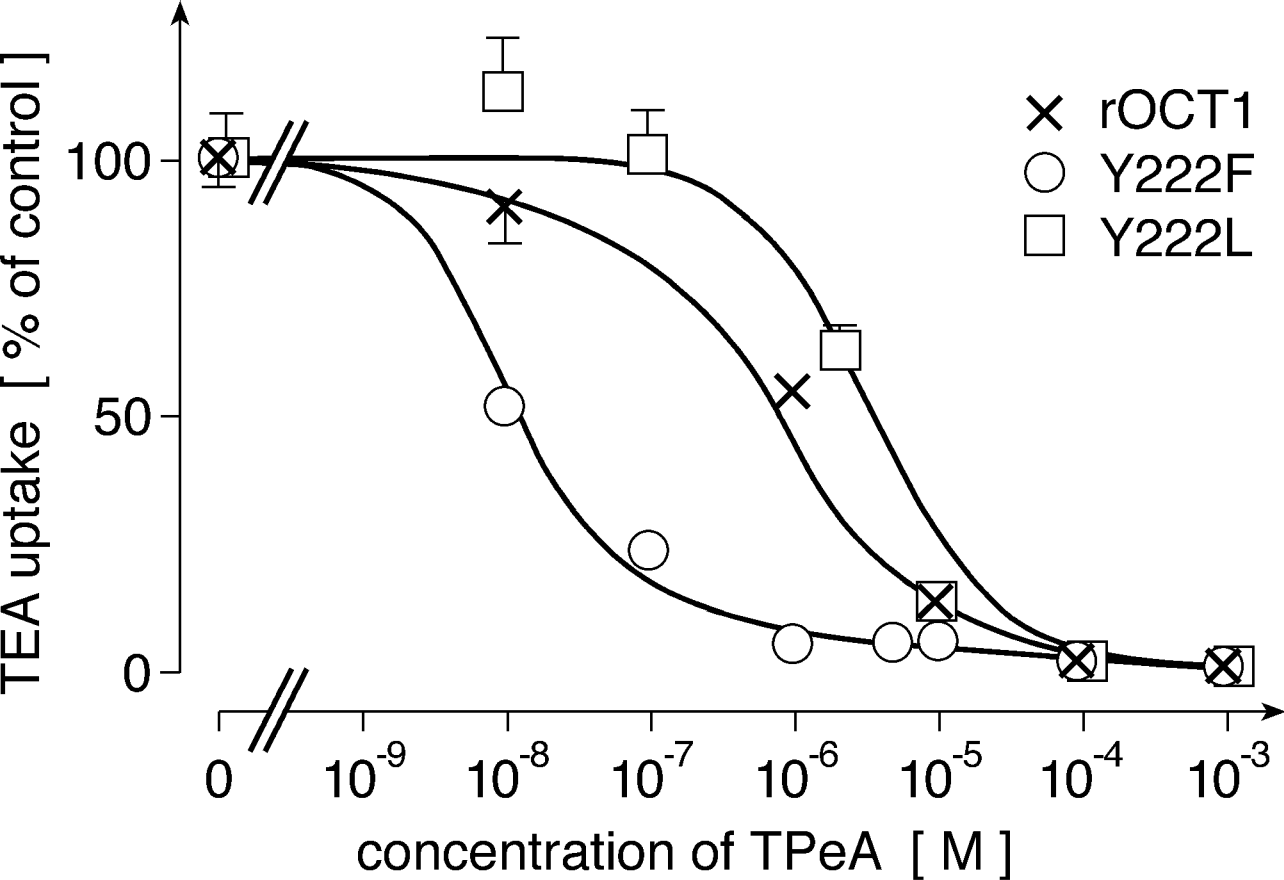


Fig. 5

	1			helix 1		52
roCT1	MPTVDDVLEQ	VGEFGWFQKQ	AFLLCLLISA	SLAPIYVGIV	FLGFTPGHY-	CQN.....
hoCT1	MPTVDDILEQ	VGESGWFQKQ	AFLLCLLISA	AFAPICVGV	FLGFTPDHH-	CQS.....
roCT2	MSTVDDILEH	IGEFHFLFQKQ	TEFLLALLSG	AETPIYVGIV	FLGFTPDHH-	CWS.....
hoCT2	MPTTVDDVLEH	GGEFHFFQKQ	MFLLALLSA	TEFPIYVGIV	FLGFTPDHR-	CRS.....
roCT3	MPTFDQALRK	AGEFGRFQRR	VFLLCLLTVG	TEAFLFVGVV	FLGSQPDYYW	CRG.....
hoCT3	MPSFDEALQR	VGEFGRFQRR	VFLLCLLTVG	TEAFLFVGVV	FLGTQPDHYW	CRG.....
LacY		MYYLKNT	NEWMFGLFFF	FYFFIMGAYF	PFPIWLHDI	N.....

	146		helix 2		helix 3	201
roCT1AWKVDL	FQSCVNLGFF	LGSLVVGZIA	DRFGRKLCLL	VTTLVTSVSG	VLTAVAPDYT
hoCT1SWKLDL	FQSCNLAGFF	FGSLGVGYFA	DRFGRKLCLL	GTVLVNAVSG	VLMAFSPNYM
roCT2SWMLDL	FQSVVNVGFF	IGAMMIGYLA	DRFGRKFCLL	VTILINAISG	ALMAISPNYA
hoCT2SWMLDL	FQSSVNVGFF	IGSMSIGYIA	DRFGRKLCLL	TTVLINAAG	VLMAISPTYS
roCT3AWMLDL	TQAILNLGFL	AGAFTLGYAA	DRYGRKLIVYL	ISCFGVGITG	VVVAFAPNFS
hoCT3AWMLDL	TQAILNLGFL	TGAFTLGYAA	DRYGRIVIYL	LSCLGVGVTG	VVVAFAPNFP
LacYKSDTGI	IFAATSLFSL	LFQPLFGLLS	DKLGLRKYLL	WIITGMLV-M	FAPFFIFIEG

	202		helix 4		helix 5	251
roCT1	SML-----	--LFRLLQGM	VSKGSWVSGY	TLITEFVG-S	GYRRTTAAILY	QMAFTVGLVG
hoCT1	SML-----	--LFRLLQGL	VSKGNWMAGY	TLITEFVG-S	GSRRTVAIMY	QMAFTVGLVA
roCT2	WML-----	--VFRFLQGL	VSKAGWLIGY	ILITEFVG-L	GYRRMVGICY	QIAFTVGLLI
hoCT2	WML-----	--IFRLIQGL	VSKAGWLIGY	ILITEFVG-R	RYRRTVGIFY	QVAYTVGLLV
roCT3	VFV-----	--IFRFLQGV	FGKGAWMTCF	VIVTEIVG-S	KQRRIVGIVI	QMFFTLGIII
hoCT3	VFV-----	--IFRFLQGV	FGKGTWMTCY	VIVTEIVG-S	KQRRIVGIVI	QMFFTLGIII
LacY	PLLQYNIIVG	SIVGGIYLG	CFNAGAPAVE	AFIEKVSRRS	NFEFGRARMF	GCVGWALGAS

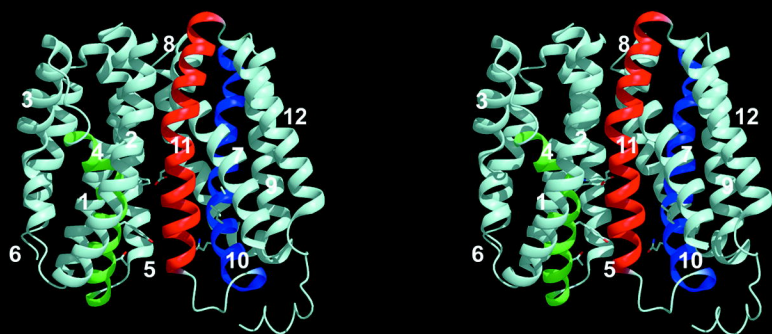
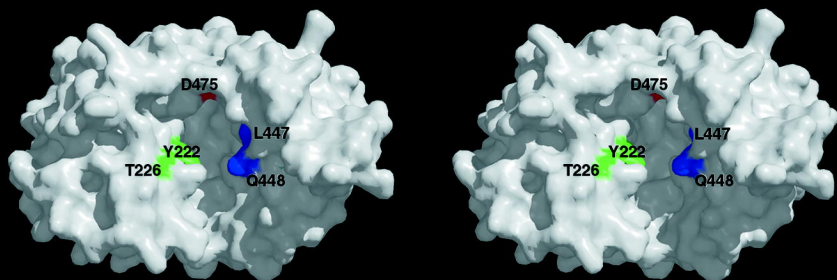
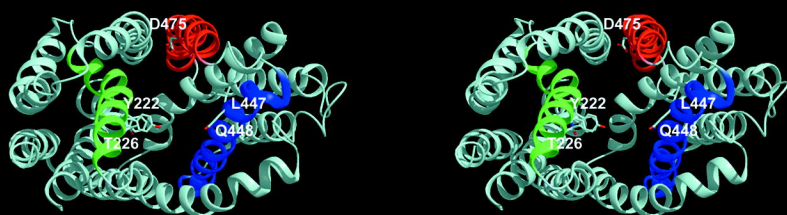
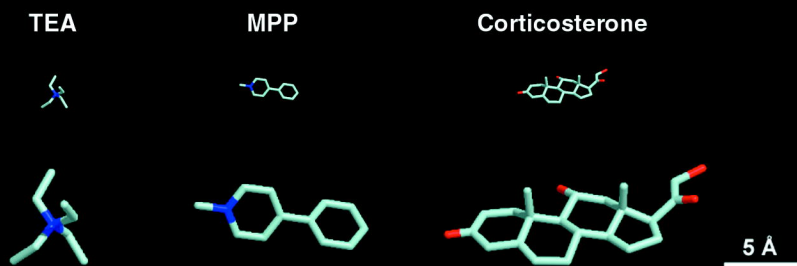
	252		helix 6		helix 7	362
roCT1	LAGVAYATPD	WRWLQLAVSL	PTFLFLLYYW	FV.....	NLRKHTVILM	YLWFSCAVLY
hoCT1	LTGLAYALPH	WRWLQLAVSL	PTFLFLLYYW	CV.....	RLRKRTFILM	YLWFTDSVLY
roCT2	LAGVAYVIPN	WRWLQFAVTL	PNFCFLLYEW	CI.....	QIRKHTLILM	YNWFTSSVLY
hoCT2	LAGVAYALPH	WRWLQFTVAL	PNFFFLLYYW	CI.....	QIRKHTMILM	YNWFTSSVLY
roCT3	LPGIAYFTPS	WQGIQLAISL	PSFLFLLYYW	VV.....	QMRKCTLILM	FAWFTSAVVY
hoCT3	LPGIAYFIPN	WQGIQLAITL	PSFLFLLYYW	VV.....	QMRKCTLILM	FAWFTSAVVY
LacY	IVGIMFTINN	QFVFWLGS	ALILAVLLEF	AK.....	KLWFLSLYVI	GVSCTYDVFD

	363		helix 8		helix 9	415
roCT1	QGLIMHVGA-	-----TGAN	LYLDFFYSSL	VEFPAAFIIL	VTIDRIGRIY	PIAASNLVTG
hoCT1	QGLILHMGA-	-----TSGN	LYLDFLYSAL	VEIPGAFIAL	ITIDRVGRIY	PMAMSNLLAG
roCT2	QGLIMHMGL-	-----AGDN	IYLDFFYSAL	VEFPAAFIIL	LTIDRVGRRY	PWAVSNMVAG
hoCT2	QGLIMHMGL-	-----AGDN	IYLDFFYSAL	VEFPAAFIIL	LTIDRIGRRY	PWAVSNMVAG
roCT3	QGLVMRLGL-	-----IGGN	LYMDFFISGL	VELPGALLIL	LTIERLGRRL	PFAASNIVAG
hoCT3	QGLVMRLGI-	-----IGGN	LYIDFFISGV	VELPGALLIL	LTIERLGRRL	PFAASNIVAG
LacY	QQFANFFTSF	FATGEQTRVF	GYVTMGELL	NASIMFFAPL	I-INRIGGKN	ALLLAGTIMS

	416		helix 10		helix 11	474
roCT1	AACLLMIFIP	HELH-WLNV	LACLGRMGAT	IVLQMVCLVN	AELYPTFIRN	LGMMVCSALC
hoCT1	AACLVMIFIS	PDLH-WLNII	IMCVGRMGIT	IAIQMICLVN	AELYPTFVRN	LGVMVCSLLC
roCT2	AACLASVFIP	DDLQ-WLKIT	IACLGRMGIT	MAYEMVCLVN	AELYPTYIRN	LGVLVCSSMC
hoCT2	AACLASVFIP	GDLQ-WLKII	ISCLGRMGIT	MAYEIVCLVN	AELYPTFIRN	LGVHICSSMC
roCT3	VSCLVAFLP	EGIP-WLRIT	VATLGRMGIT	MAFEIVYLVN	SELYPTTLRN	FGVSLCSGLC
hoCT3	VACLVTAFLP	EGIA-WLRIT	VATLGRMGIT	MAFEIVYLVN	SELYPTTLRN	FGVSLCSGLC
LacY	VRIIGSSFAT	SALEVVILKT	LHMFEVPELL	VGCFKYITSQ	FEVR--FSAT	IYLVCFCEFFK

	475		helix 12		530	
roCT1	DLGGIIFPFM	VFRLMEVWQ-	-ALPLILFGV	LGLTAGAMTL	LLPETKGVAV	PETIEEAE...
hoCT1	DIGGIITPFI	VFRLREVVQ-	-ALPLILFAV	LGLLAAGVTL	LLPETKGVAV	PETMKDAE...
roCT2	DIGGIITPFL	VYRLTDIWM-	-EFPLVVFVAV	VGLVAGALVL	LLPETKGGKAL	PETIEDAE...
hoCT2	DIGGIITPFL	VYRLTNIWL-	-ELPLMVFGV	LGLVAGGLVL	LLPETKGGKAL	PETIEEAE...
roCT3	DFGGIIPFL	LFRLAAIWL-	-ELPLIIFGI	LASVCGGLVM	LLPETKGIAL	PETVEDVE...
hoCT3	DFGGIIPFL	LFRLAAVWL-	-ELPLIIFGI	LASICGGLVM	LLPETKGIAL	PETVDDVE...
LacY	QLAMIFMSVL	AGNMYESIGF	QGAYLVLGLV	ALGFTLISVF	TLSPGGLSL	LRRQVNEV...

Fig. 6

a**b****c****d****Fig. 7**